



Challenges and opportunities in quantitative aerial thermography of building envelopes



Milad Mahmoodzadeh ^a, Voytek Gretka ^b, Phalguni Mukhopadhyaya ^{a,*}

^a Department of Civil Engineering, University of Victoria, Victoria, BC, V8W 2Y2, Canada

^b Department of Building Specialty Services, Morrison Hershfield Corp, Atlanta, GA, 30346, USA

ARTICLE INFO

Keywords:

Drone
UAV
Aerial thermography
Quantitative
Dynamic IRT
Stationary IRT
Wind
Microbolometer
Stabilization

ABSTRACT

The use of small unmanned aerial vehicles (UAVs) equipped with an infrared (IR) camera has created opportunities for qualitative and quantitative thermal assessments of building envelopes. However, it is currently unclear how successful this method is at quantifying heat losses through the building envelope. The inconsistency in findings indicates that sources of error that affect the accuracy of surface temperature measurements are not well understood by thermographers and that recommendations to minimize the errors in aerial thermography measurements have yet to be determined. In this study, laboratory and field experiments were conducted to investigate the scientific reasons for discrepancies between aerial (i.e. dynamic) and conventional stationary infrared thermography (IRT) observations. A set of practical approaches were presented to minimize the sources of error in UAV-IRT measurement. The results of field experiments showed a non-linear and dramatic variation of measured surface temperature during flight, where the deviations of results between dynamic and stationary thermography were beyond the manufacturer-reported accuracy of ± 5 °C. Additionally, the results indicated that induced convection from drone propellers affects microbolometer stabilization with surrounding environmental conditions, which significantly influences the IR camera measurement accuracy. Finally, subsequent investigations utilized a shield around the camera to minimize the convective turbulence on the lens and thermal sensors, successfully achieving temperature deviations of less than 1 °C. These findings may inform manufacturers about the limitations of current IR camera technology during aerial surveys and therefore provide opportunities to define a more robust thermal imaging protocol for the quantification of building envelope thermal performance.

1. Introduction

Infrared (thermographic) cameras were first developed for military applications [1] and became available to the commercial market in the late 1960s as bulky and cumbersome packaged equipment that required extensive cooling [2]. Current infrared (IR) cameras have improved in size efficiency but effectively follow similar physical properties and operation as their predecessors. Within the camera, a thermal detector interprets the infrared radiation emitted from a subject based on Plank's Law and the Theory of Grey Body Radiation, producing an image in the form of a colorized or greyscale temperature map [1]. The most common thermal detector in IR cameras is a microbolometer focal plane array (FPA) which works at room temperature and does not require an expensive cooling component. This method of temperature measurement, known as infrared thermography (IRT), is non-contact, non-destructive,

* Corresponding author.

E-mail addresses: miladmahmoodzadeh@uvic.ca (M. Mahmoodzadeh), vgretka@morrisonhershfield.com (V. Gretka), phalguni@uvic.ca (P. Mukhopadhyaya).

quick, and can provide real-time two-dimensional data. IRT has been used in different fields, in particular as a promising investigative tool for building envelope inspections over the last few decades [3].

Current building envelope inspections using handheld cameras are time-consuming and may require surveys from the interior as well as the exterior to fully understand the façade condition. This method of data collection provides an overview of the building envelope but often neglects smaller details and defects, which necessitates the utilization of unaided ground crews or traditional lift equipment in most cases. In other words, a comprehensive thermographic inspection of all façade elements becomes very time-consuming depending on building size and is potentially disruptive to building occupants [4]. As technology has advanced, infrared (IR) sensors have become significantly smaller and lighter, facilitating integration with unmanned aerial vehicles (UAVs) or “drones” for survey purposes, such as for building energy audits. UAVs enable professionals and researchers to rapidly analyze and identify thermal anomalies in building envelopes while reducing operations costs compared to traditional methods and minimizing the safety risks during the surveys [5]. This allows easy access to remote or inaccessible areas of a building and gives the operator unprecedented flexibility during the thermographic surveys as they are able to position the camera to overcome obstructions and reflections from nearby buildings and other radiative sources. For instance, inspections of upper floor façade elements in taller structures are otherwise only feasible with internal thermography since external IRT with a handheld camera at grade cannot provide accurate data due to the importance of distance and angle of view. However, UAVs capable of vertical take-off and landing have the ability to hover in midair and are far less restricted in their ability to collect meaningful data. In addition, when thermal anomalies are found, a UAV can be maneuvered to document it with improved resolution and to mitigate the impact of other reflections [6]. This study showcases the utilization of a UAV or “drones” mounted with a thermographic sensor for quantitative thermographic building envelope inspections, potentially for use as an energy auditing tool. The paper consists of three main sections: 1) background, which provides an overview of regulatory requirements surrounding UAV deployment in Canadian airspace as well as recently applied methodologies in the evaluation of building envelopes using aerial IRT; 2) methodology, which outlines field experiment setup and data collection procedures during aerial surveys; 3) results, which summarizes the limitations and challenges of quantitative aerial IRT measurement and; 4) conclusion, that highlights major contributions of this research and steps that can be taken to design a UAV building energy assessment survey.

2. Background

With the rapid growth of UAV applications in various industries, such as agriculture, mining, and construction, a number of regulations and policies have been developed in the interest of public safety [7,8]. These regulations include maintaining an appropriate distance from airports, providing landing spots in case of emergency, and familiarity with flight dynamics such as velocity, angle of turn, battery life and maximum control distances. In addition, obstacles such as trees, antennas, lights and surrounding buildings should be considered prior to and during the flight to avoid accidents [7–9]. Even in the context of a well-coordinated flight, human error or unforeseen circumstances may lead to UAV collisions, potentially causing human injuries. Hence, it is mandatory for the operator to maintain a liability insurance policy for their flight operations in case of injury or damage [8,9].

Due to the importance of flight planning in UAV-based studies, research studies have been conducted to detail flight planning according to industry-specific needs. In the building industry, flight procedures have been performed with full automation to record, photograph and hover at each location using an onboard Global Positioning System (GPS), a method that can further minimize the time required to conduct a survey [4]. Taher [10] compared the accuracy of GPS with ground control points informed by Google Earth Pro and found onboard GPS to be more accurate. Despite this advantage, a critical UAV flight obstacle is battery life, in particular for long flight situations (such as in the case of large buildings). Son et al. [11] suggested that pre-flight planning should be based on construction drawings or knowledge of where potential thermal anomalies exist. This method could minimize the flight time but may increase the error in determining the thermal leaks in buildings since the flight path is not based on areas of thermal anomalies. It is to be noted that more than one audit is often required to evaluate the entire building accurately due to the presence of environmental obstacles such as buildings and trees, which may obscure the façade details.

Other flight parameters such as distance to the target, flight altitude, speed, flight pattern and weather conditions are also critical considerations in thermography with UAVs [4]. Some researchers suggest various flight altitudes, ranging from 30 to 75 m above grade, in order to have a complete view, depending on the size of the building and IR camera specifications [12]. Similarly, various target distances were considered, such as 2–5 m for evaluating the damage in post-disaster areas [13] and <1 m for the identification of small cracks in concrete or masonry [14]. However, the literature is not clear regarding an ideal distance for the thermal inspection of building envelopes. Likewise, the flight path plays a key role in the quality of data collected, where researchers have suggested flying the drone either vertically or horizontally in a zig-zag pattern across the regions of interest [15–19]; Eschamann and Wundsam showed that vertical strips result in lens movement which decreases data quality image clarity, while horizontal strips were found to be ideal especially when paired with a low flight speed [19]. Apart from flight path planning, environmental parameters such as solar irradiation, sky condition, wind, and moisture could have a substantial influence on the accuracy and interpretation of results obtained from thermography. Further research activities have led to the establishment of a handful of best practices for thermographic surveys to improve the accuracy of results. Recommended solutions are 1) performing tests in stable weather [20,21]; (2) avoiding IRT surveys during rainy and sunny days [22–24], and (3) ensuring wind speed is less than 1 m/s during the measurement and free-stream wind speed is less than 5 m/s for a period of 24 h before testing [23,24].

The aforementioned procedures in the literature have provided the groundwork to use UAV-based thermography for the evaluation of building envelope thermal performance. The analysis could be performed both qualitatively and quantitatively for locating, diagnosing and quantifying areas of heat losses such as thermal bridges, air leakage, or the presence of moisture in the envelope. No-

table, investigations involving qualitative aerial thermography [7,25–28] are more numerous than quantitative studies in spite of recent advancements in stationary quantitative IRT. Interestingly, the accuracy of findings and conclusions in quantitative aerial IRT investigations differed on a case-by-case basis, which can be attributed to the differing performance of IR cameras in flight conditions and the expertise of thermographers. For example, Bayomi et al. [29] presented the advantage of aerial thermography in quantifying the U-value of the building envelope for input to a building energy model. The results indicated that the accuracy of simulation results was improved when the U-value determined by aerial IRT was used. In contrast, Kelly et al. [30] indicated that the measured temperature by aerial thermography was not stable during the flight due to varying ambient conditions and the camera's temperature, where the camera performance during the flight was completely different ($\pm 0.5^{\circ}\text{C}$) relative to laboratory conditions ($\pm 0.5^{\circ}\text{C}$).

Likewise, Krishna Ribeiro-Gomes et al. [31] illustrated that temperature accuracy is limited during the aerial IRT due to the temperature instability of the camera's thermal detector during flight. To address this issue, the author proposed a calibration algorithm based on a neural network to minimize the effect of the sensor's temperature on the measurement. The proposed methodology reduced the measurement error to approximately 1.5°C . Nonetheless, the findings of Smigaj et al. [32] on the performance of an uncooled IR camera during flight indicated that the variations of ambient conditions during the take-off do not have a significant effect on the accuracy of thermal imagery. This contrasting result may have been caused by not exposing the camera to sustained wind, or the camera did not experience a drastic change in its temperature during the experiment.

Zheng et al. [33] conducted an experimental study to develop a 3D point cloud model for evaluating the thermal performance of a building envelope using UAV-IRT. The results showed that dynamic IRT measurements in an ideal environment differed by $\pm 5^{\circ}\text{C}$ at selected points compared to the thermocouple contact measuring method. Also, the authors found that the error in measurement gradually decreased over time (~20 min), suggesting the extent of IR camera stability with its surrounding environment may impact measurement accuracy. However, a recent study by Dabutar et al. [34] on the development of a 3D point cloud model using aerial thermography for detecting sources of heat losses in a building did not have the same IR camera stability issue observed in the Zheng et al. [33] study.

Given the inconsistency in findings, it may be deduced that the factors and sources of error that impact the measurement accuracy are more complex and may not be well understood. Also, practical approaches to minimize measurement error have not yet been developed; therefore, the inaccuracy of measurements cannot help decision makers to prioritize building envelope retrofits from a performance perspective. Hence, it is imperative to understand the scientific reasons behind limitations and develop robust and reliable data acquisition procedures.

To address the current gap in the literature, this study intends to demonstrate the performance of IR camera during the flight and indicate how a robust measurement can be obtained for the utilization of aerial thermography in building envelope thermal performance assessments. This goal is addressed in this study through the following objectives: first, the viability of dynamic measurements relative to stationary measurements (handheld camera) for quantitative thermal assessment of building envelopes is examined. Second, the scientific reasons for discrepancies between measurements are illustrated. Finally, a set of practical approaches to maximize measurement accuracy in aerial thermography are presented. The findings from this study will be valuable for thermographers and researchers to develop a robust protocol that accounts for the impacts of the camera's performance.

3. Materials and methods

For this study, a set of field and lab experiments were designed and performed to achieve the objectives of the research. First, the performance of the IR camera during flight relative to the stationary measurements was assessed. Second, the effect of drone distance from the wall on measurement accuracy was evaluated, and the challenges associated with the flight, such as the sensitivity of the camera's response due to varying ambient conditions, were examined. Third, the required time for the camera to stabilize during the flight was determined. Finally, a practical approach to minimize sources of error during the flight was introduced, and recommendations as a protocol for quantitative aerial thermography were provided. The experimental setup is described in this section, followed by a more detailed explanation in the Results section. It should be noted that the design and sequence of experiments were influenced by the results obtained in the previous phases.

3.1. Case study and measuring instruments

Experiments were performed from the outside on an insulated and conditioned wood-framed structure. The structure has an area of 9.30 m^2 and a ceiling height of approximately 3.05 m. The plan view and cross-section of the structure are available in Ref. [23]. The wall considered in the analysis is facing north and incorporates a double-glazed operable (sliding) window (Fig. 1). The equipment for this study included two IR cameras, a drone, an oil-filled electric radiant heater, temperature sensors with an accuracy of $\pm 0.01^{\circ}\text{C}$ integrated with a data logger, and an anemometer to measure wind speed (accurate to $\pm 0.1\text{ m/s}$). All equipment was calibrated before the tests according to manufacturers' specifications. Indoor air temperature was controlled with a portable oil-filled electric radiant heater connected to a thermostat set to 22°C . Two thermal cameras were considered to measure the surface temperature of the wall. The first one was the FLIR Zenmuse XT2 IR camera which is specially designed to be mounted on the drone (Fig. 2). The aerial surveys were performed with a DJI Matrice 200 Series drone, which has vision systems located on the front and bottom of it, including stereo vision sensors and two ultrasonic sensors. The vision systems allow the aircraft to avoid collisions with obstacles during hovering. In addition, there is an infrared sensing system consisting of two infrared modules on top of the drone, which scans the obstacles on the top side of the drone. The use of a remote pan and tilt system allows the camera to be oriented at the desired angle to the target to enhance measurement accuracy. The operator controlled the movements of the gimbal and camera operation with a



Fig. 1. The experimental structure, showing the wall considered for analysis.



Fig. 2. Images of the drone with mounted Zenmuse XT2.

remote controller during the surveys. It is to be noted the drone's operation followed the regulations and policies within Canadian Air-space.

The second IR camera was FLIR A65, which is a conventional hand-held IR camera. It was considered to compare and evaluate the measurements with aerial IRT. Both cameras use an uncooled VOx microbolometer FPA with a 640×512 pixel focal plane array detector. The Zenmuse XT2 has a 19 mm lens, leading to a narrower field of view relative to the A65 with a 13 mm lens. This results in more pixels of the target, improving thermal anomaly detection potential. The thermal cameras provide an accuracy of $\pm 5^\circ\text{C}$ under ideal environmental conditions, implying that their measurements are comparable. Camera specifications are shown in [Table 1](#) and [Fig. 3](#).

Table 1
Technical specifications of IR cameras.

Model	Resolution (Pixels)	Thermal sensitivity	Field of view	IFOV	Spectral Band	Accuracy
DJI Zenmuse XT2	640×512	0.05°C	$32^\circ \times 26^\circ$	1.3 mrad	7.5–13.5 μm	$\pm 5^\circ\text{C}$
FLIR A65	640×512	0.05°C	$45^\circ \times 37^\circ$	0.9 mrad	7.5–13 μm	$\pm 5^\circ\text{C}$



Fig. 3. IR cameras; (a) Zenmuse XT2 (drone-mounted camera); (b) FLIR A65 (handheld camera).

3.2. Measurement setup and data acquisition procedure

The drone location was pre-determined with a flight altitude of 3 m above grade, and its distance from the target was 8 m to ensure the entire wall was in the field of view of the camera. To ensure a safe flight, the presence of obstacles such as power lines, trees and adjacent buildings was observed prior to the experiments. The handheld camera was mounted on a tripod at the same distance from the wall (Fig. 4). The spot size ratios were measured to ensure the cameras are capable of accurately measuring the temperature at the proposed distance. A minimum spot size ratio of 18 mm is required for the gross thermal patterns around insulation, significant thermal bridges, and air leakage [23,24]. According to the cameras' specs and the distance, spot size ratios of 7.2 mm and 10 mm were obtained for Zenmuse XT2 and FLIR A65, respectively. In addition, to study the effect of forced convection due to drone-induced wind on the wall surface, a subsequent experiment was also considered at a distance of 2 m from the wall. Finally, to mimic the field performance of the camera during the flight, a time series lab experiment was conducted to investigate the required time for camera stabilization during flight (Further details are in Section 4.2).

A region of interest (ROI) was considered around the center of thermal images to avoid the vignetting effect, an artefact where corners appear colder than the center of the thermal image [23,24]. It is to be noted that during the post-processing, the mean value of pixels in the ROIs was considered due non-uniformity of pixels' sensitivity to the incoming radiation from the object. To ensure the stability of environmental conditions during the surveys, both dynamic and static measurements were performed at the same time and distance in a direction perpendicular to the wall. Also, to appreciate the performance drone IR camera during the flight, measurements were collected temporally (1 frame/second).

Environmental conditions such as solar radiation, wind speed, rain, sky conditions, and temperature gradient were observed during the days prior to the thermal inspection and on the inspection day. The wall was not exposed to rain or snow 48 h prior to the tests, and the sky was cloudy before (~ 12 h) and during the tests. The indoor air temperature was approximately constant before and during the tests, and the outdoor air temperature was stable a few hours prior to the tests. A minimum temperature difference of 15 K was maintained during the surveys, and the measured wind speed was lower than 1 m/s. Emissivity and reflected apparent temperature for calibration of IRT measurement were measured prior to each test by each camera according to the established standards, which have been elaborated in previous studies [26,27]. Finally, FLIR ResearchIR software was used to perform further analysis on thermal images (post-processing), with functionality to change temperature span, color palette, adjustments to parameters such as emissivity, reflected temperature, ambient air temperature, humidity, air transmission coefficient, and distance of the camera to target. A flowchart describing the procedure of experiments is illustrated in Fig. 5.

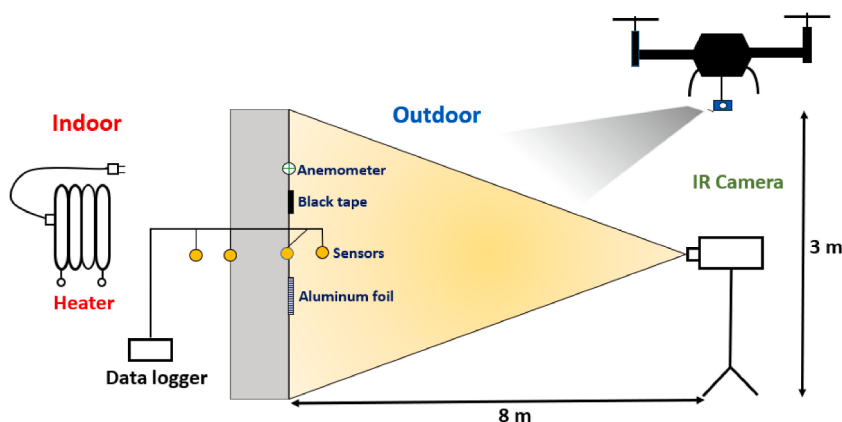


Fig. 4. Schematic of experimental setup.

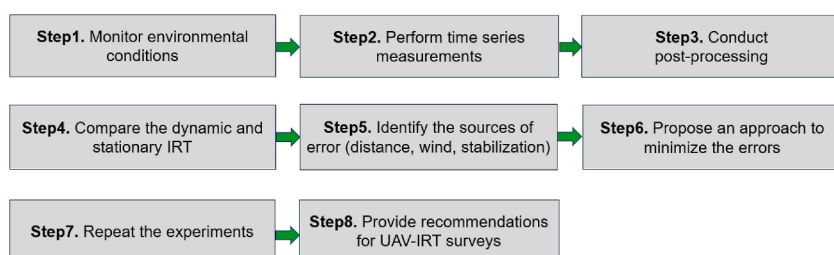


Fig. 5. Study analysis flowchart.

4. Results and discussion

To clarify the importance of each step of the methodology (shown in Fig. 5), the results were presented in four sections. The sections include: first, a comparison between the accuracy of aerial and stationary quantitative IRT for surface temperature measurement of a wall assembly (section 4.1); second, understanding the causes of temperature drift in aerial thermography and their impact on the accuracy of measurement as compared to stationary measurements (section 4.2); third, mimicking the flight conditions in a laboratory environment as a consequence of limited drone battery life, which was too short to determine the required camera's thermal detector stabilization time in flight to ensure the recorded temperature is stable (section 4.3), and finally, developing an in-situ approach based on findings in previous steps to minimize error during quantitative aerial thermography of building envelopes (section 4.4).

4.1. Dynamic vs. stationary IRT

The results in Fig. 6 are based on a survey on a cloudy day where the wind speed was about 0.60 m/s, and the indoor and outdoor temperatures were 22.12 °C and 7.22 °C, respectively. Substantial deviations between surface temperature measurements with FLIR Zenmuse XT2 (airborne) and FLIR A65 (stationary) were observed during the test. Unexpectedly, the drone measurement showed a temperature below 0 °C, which was completely different from measurements obtained with stationary IRT. Also, the measured temperature gradually decreased from −8.31 °C to −24.42 °C after ~10 min while the drone was hovering. As illustrated in Fig. 6, the measurement with the drone-mounted camera was about −24 °C (Box 1), while the surface temperature (Box 2) measured with the stationary camera was almost 8 °C. To ensure the validity of measurements, several tests were performed on different days, yielding a similar trend.

Considering these results, it was assumed that the Zenmuse XT2 IR camera does not have a good performance during the flight. However, due to the possibility of dynamic measurement uncertainty, it was decided to perform a static (grounded) measurement with the drone-mounted Zenmuse XT2 to understand the potential confounding effects of flight. The drone was placed on a tripod, and its propellers were turned off while thermal images were taken with its mounted camera. Results were more representative than the dynamic in-flight case (−4.52 °C vs −24.42 °C), suggesting major interference from flight operation, likely from convective cooling effects induced by drone propellers on the camera (Fig. 7). In addition, it was likely that the effect of varying outdoor environmental conditions may not have been considered in the reported camera's accuracy by the manufacturer. Discussions with the manufac-

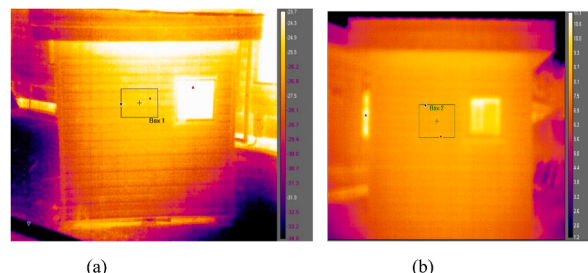


Fig. 6. Thermal images obtained with (a) drone-mounted camera (Zenmuse XT2) in-flight with negative color scale; (b) handheld camera (FLIR A65) with positive color scale. (For interpretation of the references to color in this figure legend, the reader is referred to the Web version of this article.)



Fig. 7. Thermal images obtained with grounded drone-mounted Zenmuse XT2 (propellers off).

turer confirmed that the temperature measurement accuracy of the Zenmuse XT2 can be affected by environmental factors since its accuracy ($\pm 5^\circ\text{C}$) was obtained under ideal environmental conditions (lab), not flight conditions. This was confirmed during the calibration process, where surface temperature measurements of a target with a known temperature under lab conditions for both IR cameras were relatively similar (deviation of $\sim 0.51^\circ\text{C}$) and within the range of their accuracy; therefore, it was confirmed that outdoor environmental conditions significantly affect the performance of Zenmuse XT2. This unexpected observation necessitates further investigation, which is detailed in the following sections.

4.2. Analysis of inconsistencies in camera output- sources of error

The temporal variations in temperature observed in the previous section were not justifiable since wall surface temperature is not likely to have changed dramatically in a short period of time (~ 3 min), given the stability of environmental conditions at the time of the test. Therefore, three possible explanations were considered for these deviations. First, the Zenmuse XT2 is not accurate enough for quantitative measurements and should be limited to qualitative measurements such as identifying locations of hot spots or large thermal contrasts (i.e., detecting wildfires where a deviation of $10\text{--}20^\circ\text{C}$ does not affect the conclusion of investigations). Second, the induced wind by the drone's propeller influences the performance of the IR camera (unstable environmental conditions around the camera) and consequently affects surface temperature measurements. Finally, depending on the distance of the camera to the target, induced wind from the drone flight may increase convection heat transfer on the wall surface, thereby magnifying surface temperature reduction. To this end, due to the reliability and better accuracy of static measurements with the handheld IR camera (FLIR A65), it was decided to mount this camera on the drone instead to understand dynamic accuracy in the presence of other factors (i.e., wind, ambient temperature, convection, distance).

A test (Case 1) was performed on a cloudy night where the wind speed was about 0.10 m/s , and indoor and outdoor temperatures were 24.22°C and 9.24°C , respectively. The IR cameras were warmed up for almost 30 min prior to the test to stabilize the IR camera microbolometer with ambient temperature. Before the dynamic measurement, a time series static measurement was performed for validation purposes (Fig. 8). The dynamic measurements were conducted at two distances from the target (2 m and 8 m) to study the effect of forced convection on the wall surface due to drone-induced wind (Fig. 9). Thermal images were recorded continuously for ~ 15 min, with a data acquisition interval of 1 s for each distance while the drone was hovering. The results of time series dynamic (blue line) and static (orange line) measurements belonging to Box 1 in Fig. 9 are shown in Figs. 10 and 11. It is seen that the temperatures decreased over time (dropped to 3.53°C), similar to the trend exhibited by the Zenmuse XT2, and were lower than stationary measurements. However, the accuracy of measurement was substantially better than Zenmuse XT2 since temperatures (1) were above

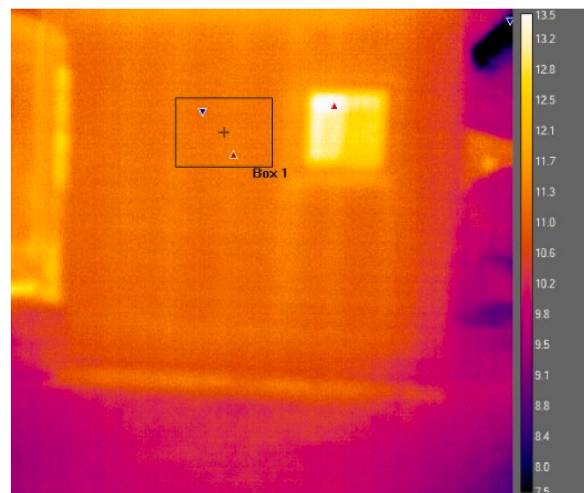


Fig. 8. Stationary thermal image taken before dynamic measurement with drone.

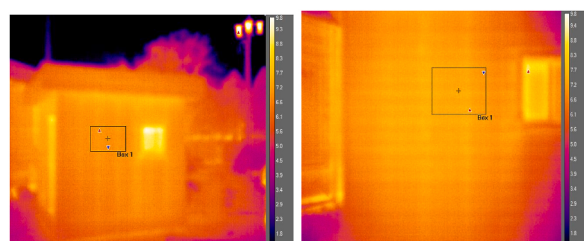


Fig. 9. Thermal images taken with drone-mounted FLIR A65; (a) at distance of 8 m; (b) at distance of 2 m.

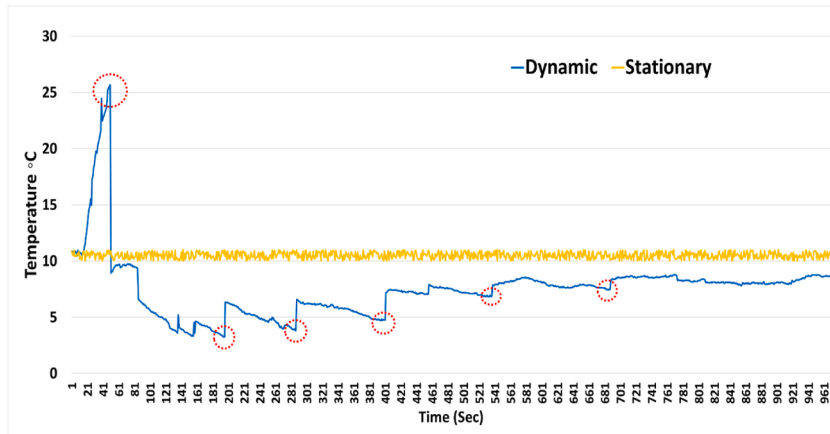


Fig. 10. Dynamic (in-flight) thermal imaging with drone-mounted FLIR A65 at a distance of 8 m from the wall surface; Static measurement (orange line); Dynamic measurement (blue line); Activation of NUC (red circles). (For interpretation of the references to color in this figure legend, the reader is referred to the Web version of this article.)

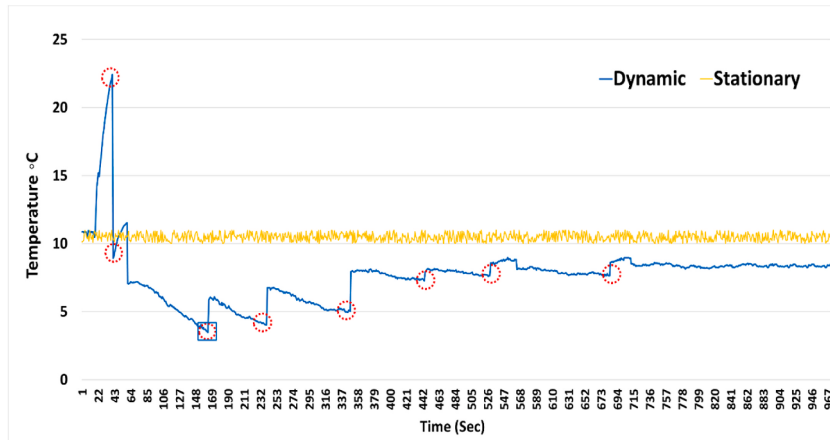


Fig. 11. Dynamic (in-flight) thermal imaging with drone-mounted FLIR A65 at a distance of 2 m from the wall surface; Static measurement (orange line); Dynamic measurement (blue line); Activation of NUC (red circles). (For interpretation of the references to color in this figure legend, the reader is referred to the Web version of this article.)

0 °C, and (2) stabilized during the test (after ~14 min). Interestingly, the drone's distance to the target did not markedly influence the accuracy of measurements: temperature variation trends were almost identical for both distances studied, in spite of wind speed differences at the wall surface (about 1.52 m/s and 0.11 m/s at a drone distance of 2 m and 8 m, respectively). In other words, variations in convective heat transfer did not affect results. This finding suggests that drones may be able to get into close proximity to a building envelope to detect small defects or air leakage using IRT, without compromising results.

Figs. 10 and 11 also show a dramatic increase in temperature measurement shortly after take-off. This camera behaviour can be attributed to a sudden change in surrounding environmental conditions created by drone-induced wind, where internal components of the camera are overcompensating before the non-uniformity correction (NUC) function is activated (red circles). In other words, the camera experiences sudden changes where the rate of NUC activation (interval between NUCs) might be slower than environmental changes around the camera. This behaviour is similar to the findings of Kelly et al. [30]. Since the microbolometer in an uncooled IR camera works at ambient temperature, any variation in ambient conditions around the camera would result in temperature variations of the camera's interior and focal array plane (FPA), and eventually affect temperature measurement, consistent with observations reported in the literature [3,30]. However, the temperature dependency of a camera's sensor is unknown. As suggested by Budzier et al. [35], some IR camera manufacturers use a predictive model which estimates the expected temperature of the camera interior based on its previous temperature variations. This may explain the over-compensation when the exterior and interior temperature of the camera experiences larger temperature differences than those which have previously occurred in stable conditions. These findings were consistent with observations reported by Kelly et al. [30] and Budzier et al. [35], where inconsistencies in camera output were explained during the take-off; the camera's temperature had an inverse correlation with temperature measurements.

After take-off and activation of the NUC function, the temperature measurement dropped to a lower magnitude than the stationary measurement highlighting the influence of drone-induced wind. To illustrate this in more detail, the variation of ambient temperature

due to cooling effect of wind influences the stability of the focal plane array (FPA) temperature, which results in temperature drift. The temperature of the FPA is influenced by ambient air temperature since the lens of the camera is exposed to wind and the thermal conductivity from the lens to the FPA is high. Hence, due to the instability of the FPA temperature, further time is required for the FPA to reach thermal equilibrium. It should be noted that this time depends on the camera housing's heat dissipation characteristics which affect the magnitude of the temperature difference between the FPA and the ambient air temperature [3].

The spikes in temperature measurement at different intervals indicate the activation of NUC to harmonize signal response across the sensor. The non-uniformity correction (NUC) in the IR camera should be applied more frequently during aerial measurements than during stationary measurements to reduce the temperature drift. As illustrated in Figs. 10 and 11, the difference between dynamic and static measurement decreases as the camera stabilizes with ambient air temperature. In both scenarios, the temperature almost converged with initial values after approximately 14 min. However, IRT-UAV data collection was limited by its almost 20-min battery life, which was insufficient for complete camera stabilization. It should be pointed out that it is not recommended to run the drone at its maximum battery life (20-min), and this is why the tests were performed for almost 14 min.

4.3. Stabilization time-lab experiment

In the previous section, it was found that camera stabilization affects the accuracy of measurements. Thus, due to a limited drone battery life, it was decided to perform a lab-based experiment to determine the required time for camera stabilization (indoor temperature of 25.46 °C). Schematic of the lab experimental setup for the required stabilization time is shown in Fig. 12. In this experiment, a fan was positioned at a distance of 20 cm from a stationary IR camera while the surface temperature of the lab wall was recorded every second. A wind speed of ~4 m/s on the camera was measured with an anemometer to mimic the flight condition (drone-induced wind). As shown in Fig. 13, a rapid increase in temperature measurement was observed because of a sudden induced wind around the camera, a similar trend to the one observed in the flight experiment. However, after activation of the first NUC, the temperature dropped to 24.63 °C and, after that, fell to 17.78 °C. This is consistent with earlier findings during the flight where the FPA had not yet reached thermal equilibrium at the beginning of the flight. However, after about 20 min, the temperature approached its initial reading, converging to a nominal 0.54 °C temperature difference. This confirms the necessity of additional time for the stabilization of FPA to improve measurement accuracy. However, because of constraints on flight time due to limited battery power and is-

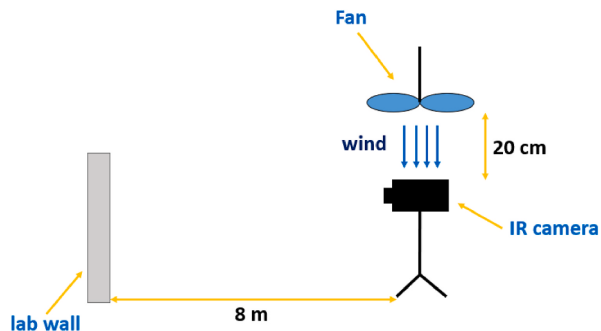


Fig. 12. Schematic of lab experimental setup for required stabilization time.

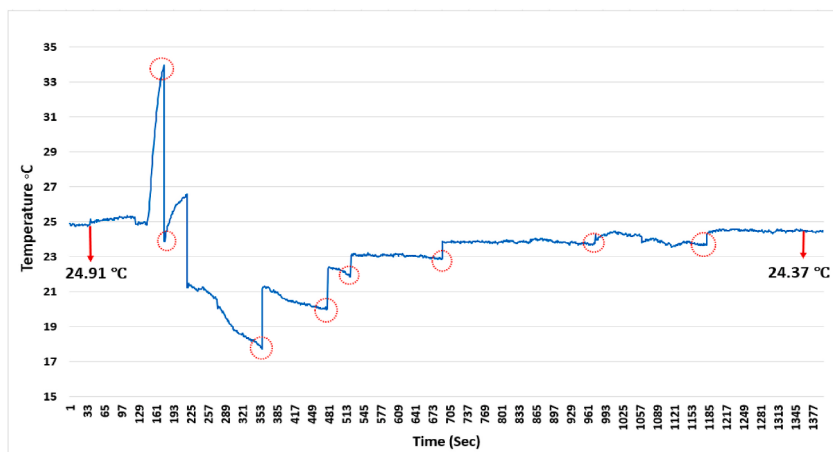


Fig. 13. Temporal variation of surface temperature measurements in the lab; stationary IR camera exposed to fan-induced wind; Activation of NUC (red circles). (For interpretation of the references to color in this figure legend, the reader is referred to the Web version of this article.)

sues with powering the camera during flights, an extra flight time of 20 min or more may not be feasible despite reducing temperature drift.

4.4. Field calibration in aerial IRT

The required stabilization time demonstrated in the lab experiment (more than 20 min) necessitated the development of an alternative approach to minimize the impact of wind during flight. Hence, a plexiglass windshield was fabricated around the IR camera with a small opening for the lens (shown in Fig. 14). A test flight (Case 2) for data collection was performed on a cloudy day where the indoor and outdoor temperatures were 24.42 °C and 9.12 °C, respectively. It was found that temperature measurements decreased during take-off, unlike the experiment that did not employ a windshield, which confirmed that the impact of wind on the performance of the camera is significant. Nonetheless, temperature deviations between stationary and dynamic conditions persisted (Fig. 15). One possible explanation for this finding is that air turbulence around the camera influences the exposed lens and, consequently, the microbolometer stability. Similar to the previous condition, the temperature measurement became more stable, and deviations became smaller. From this experiment, the following key findings were found. First, the shield mitigates camera overcompensation (an increase in temperature) during take-off. Second, the shield does not have a substantial effect on IR camera stabilization, and the IR camera stabilization depends on the extent of lens exposure to surrounding environmental conditions. Finally, to improve results, the lens should be shielded from turbulent air as much as possible.

At the time of the survey, a cylinder was positioned around the lens (Case 3) to minimize the effect of turbulence on the lens of the camera (Fig. 17). From the resulting temperature measurements shown in Fig. 16, it can be seen that the temperature reduction was substantially smaller than scenarios without a cylindrical lens shield. Also, the temperature stabilized much faster than in scenarios without a cylindrical lens shield, and the deviation between the stationary and dynamic temperature measurements was considerably lower than scenarios without a cylindrical lens shield (less than 1 °C). It can therefore be concluded that since the lens was less exposed to turbulent air, its internal temperature deviation was mitigated, and the camera stabilized faster.

The applicability of the proposed method could be illustrated based on two terms: 1) science and technology. In terms of science, the development of standard procedures and methodology ensure accuracy and efficiency in the energy assessment of buildings. For instance, reducing the error in measurement provides opportunities for accurate measurement of building envelope thermal transmittance (U-value), which is one of the main uncertain inputs in energy models. Using actual U-value in building energy models can result in a better estimation of building energy performance and, consequently, more accurate conclusions concerning the cost-benefit trade-offs of potential envelope retrofits. In terms of technology, the proposed study would inform the manufacturers and researchers about the limitations of the current design in IR cameras during flight as well as the importance of IR cameras' performance in both



Fig. 14. Prototype wind shield around the IR camera.

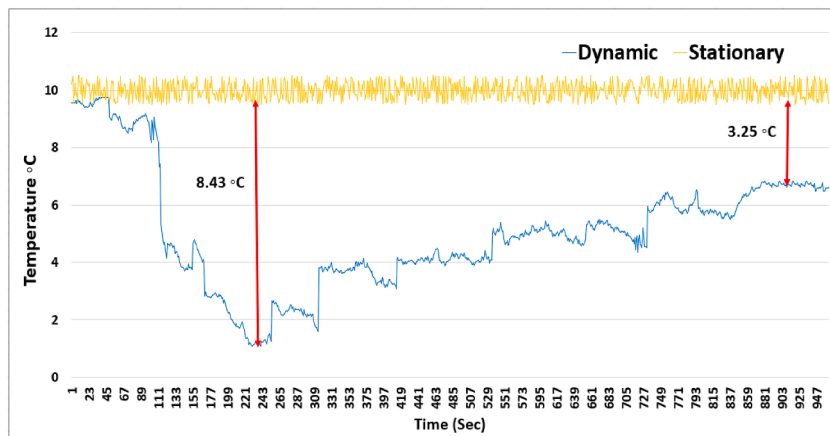


Fig. 15. Temporal variation of surface temperature measurements with IR camera shielding; Static measurement (orange line); Dynamic measurement (blue line). (For interpretation of the references to color in this figure legend, the reader is referred to the Web version of this article.)

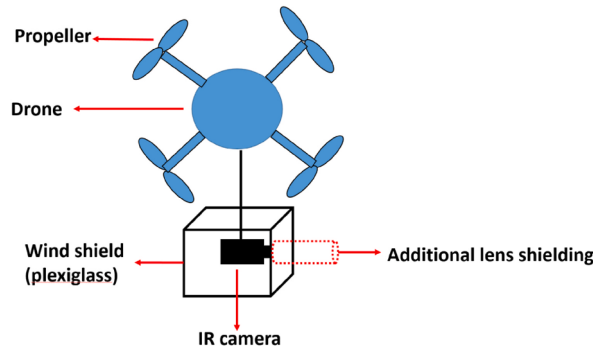


Fig. 16. Schematic of additional lens shielding.

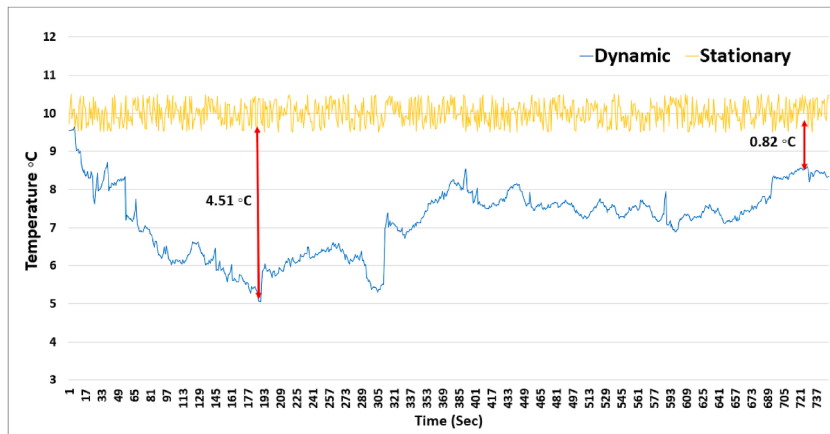


Fig. 17. Temporal variation of surface temperature measurements with a camera and additional lens shielding; Static measurement (orange line); Dynamic measurement (blue line). (For interpretation of the references to color in this figure legend, the reader is referred to the Web version of this article.)

lab and field conditions to ensure a balanced performance in any environmental conditions. Eventually, the advancement in technology yields more accurate results and provides opportunities for automated surveys, stability enhancement, accessibility and increased accuracy of aerial surveys.

5. Conclusions

In this study, dynamic IRT surveys using unmanned aerial vehicles (UAVs) or “drones” were conducted on an insulated wood-framed wall assembly to evaluate the challenges and opportunities of dynamic measurements for quantitative assessments of building envelope thermal performance. The results of dynamic IRT measurements were compared with stationary measurements during the surveys. Further, field experiments were conducted to test the response of IR cameras under changing ambient conditions. Finally, sources of error were analyzed, and a set of practical approaches were developed to minimize the severity of errors in aerial thermography.

The results demonstrated a non-linear and dramatic variations of temperature (camera response) during the flight due to varying ambient conditions, unlike stationary IRT. The findings of this investigation are in line with observations reported by Kelly et al. [30]. The deviations of results between dynamic (Zenmuse XT2 camera) and stationary thermography (FLIR A65 camera) were substantial (beyond the cameras’ reported accuracy of $\pm 5^{\circ}\text{C}$), implying that dynamic IRT measurements are not as accurate as stationary measurements. As observed from the results of this study, the thermal sensor is affected by drone propeller-induced wind during the flight, resulting in sensor temperature instability that subsequently affects the accuracy of results. However, the drone’s distance from the target did not markedly influence the accuracy of measurements; variations in convective heat transfer on the wall induced by the drone propellers did not affect results. Notably, the deviation of dynamic and stationary measurements decreased over time ($\sim 8^{\circ}\text{C}$ at the beginning of flight vs. $\sim 2^{\circ}\text{C}$ at the end), suggesting that as the sensors stabilize with environmental conditions during flight, i.e., the accuracy of results improves. This was consistent with findings reported by Kelly et al. [30] and Zheng et al. [33].

In summary, the results at different stages of this research aided to develop practical approaches and recommendations that should be considered for generating robust data from aerial thermography. Firstly, it is recommended, similar to the stationary IRT, the environmental conditions such as solar radiation, wind speed, rain, sky conditions, and temperature gradient should be observed during the days prior to the thermal inspection and on the inspection day. This can be done by performing the surveys under cloudy skies, low wind speeds (less than 1 m/s), avoiding surveys when the envelope is exposed to solar radiation, rain and snow, and ensur-

ing a minimum temperature difference of 15 K between inside and outside. Secondly, IR cameras should be warmed up for almost 30 min prior to the test to stabilize the IR camera's microbolometer with the temperature of ambient air. Thirdly, non-uniformity correction (NUC) should be applied much more frequently during dynamic measurements than in stationary measurements to reduce temperature drift. Finally, to minimize the effect of sudden turbulence around the camera during flight, it is suggested to shield the camera as much as possible, particularly the lens. Due to the duration of aerial surveys being limited by battery life, a shield facilitates faster camera stabilization, consequently allowing for more data collection per flight. Observations further showed that the aforementioned practical approaches and recommendations could help decreasing the deviation between dynamic and stationary measurements to less than 1 °C.

This work is one of the first steps toward a highly automated and reliable method for inspecting and quantifying a building envelope's thermal performance. Although the implications of UAV for qualitative thermal assessment of building envelopes have been widely studied, more research is required to develop a robust protocol for quantitative thermal assessment of building envelopes. The future work of this investigation will focus on the development of robust protocols to enhance the accuracy of dynamic surveys. Furthermore, the limitations and suggestions in this study require further study on various IR camera technologies. It should be remarked that enhancement of this limitation requires further attention and investigation from researchers and manufacturers towards improving the technology of IR cameras for aerial surveys similar to that of a stationary one.

Credit author statement

Milad Mahmoodzadeh: Conceptualization, Methodology, Software, Investigation, Validation, Writing - original draft, Visualization, Formal analysis. **Voytek Gretka:** Conceptualization, Methodology, Validation, Visualization, Formal analysis, Writing - review & editing. **Phalguni Mukhopadhyaya:** Conceptualization, Supervision, Project administration, Funding acquisition, Writing - review & editing.

Declaration of competing interest

The authors declare that they have no known competing financial interests or personal relationships that could have appeared to influence the work reported in this paper.

Data availability

No data was used for the research described in the article.

Acknowledgment

Authors would like to acknowledge the support of NSERC, MITACS, BC Housing, CBBI, CFI, BCKDF and Morrison Hershfield Ltd. for providing financial and/or technical support for this research initiative.

References

- [1] C. Meola, G.M. Carlomagno, Recent advances in the use of infrared thermography, *Meas. Sci. Technol.* 15 (9) (2004) R27–R58, <https://doi.org/10.1088/0957-0233/15/9/r01>.
- [2] M. Fox, D. Coley, S. Goodhew, P. de Wilde, Thermography methodologies for detecting energy related building defects, *Renew. Sustain. Energy Rev.* 40 (2014) 296–310, <https://doi.org/10.1016/j.rser.2014.07.188>.
- [3] B. Aragon, K. Johansen, S. Parkes, Y. Malbeteau, S. Al-Mashharawi, T. Al-Amoudi, C.F. Andrade, D. Turner, A. Lucieer, M.F. McCabe, A calibration procedure for field and UAV-based uncooled thermal infrared instruments, *Sensors* 20 (11) (2020) 3316, <https://doi.org/10.3390/s20113316>.
- [4] T. Rakha, A. Gorodetsky, Review of unmanned aerial system (UAS) applications in the built environment: towards automated building inspection procedures using drones, *Autom. Construc.* 93 (2018) 252–264, <https://doi.org/10.1016/j.autcon.2018.05.002>.
- [5] L.E. Mavromatidis, J.L. Dauvergne, R. Saleri, J.C. Batsale, First experiments for the diagnosis and thermophysical sampling using impulse IR thermography from Unmanned Aerial Vehicle (UAV), in: *Proceedings of QIRT Conf., 2014*, pp. 1–8 Bordeaux, France.
- [6] L. Ma, M. Li, L. Tong, Y. Wang, L. Cheng, Using unmanned aerial vehicle for remote sensing application, in: *21st International Conference on Geoinformatics, 2014 Kaifeng*.
- [7] Ann Cavoukian, *Privacy and Drones: Unmanned Aerial Vehicles, Information and Privacy Commissioner of Ontario, Ontario, 2012 Canada*.
- [8] A.G. Entrop, A. Vasenev, Infrared drones in the construction industry: designing a protocol for building thermography procedures, *Energy Prog.* 132 (2017) 63–68, <https://doi.org/10.1016/j.egypro.2017.09.636>.
- [9] Jed Chong, Nicole Sweeney, *Civilian Drone Use in Canada, Library of Parliament = Bibliothèque du Parlement, 2017*.
- [10] K.N. Tahar, Aerial terrain mapping using unmanned aerial vehicle approach, *ISPRS - Int. Archiv. Photogram. Rem. Sens. Spatial Inform. Sci.* (2012) 493–498 <https://doi.org/10.5194/isprarchives-xxxix-b7-493-2012>, XXXIX-B7.
- [11] H. Son, S. Lee, C. Kim, Automated 3D model reconstruction to support energy-efficiency, *Procedia Eng.* 145 (2016) 571–578, <https://doi.org/10.1016/j.proeng.2016.04.046>.
- [12] T.D. Stek, Drones over Mediterranean landscapes. The potential of small UAV's (drones) for site detection and heritage management in archaeological survey projects: a case study from Le Pianelle in the Tappino valley, Molise (Italy), *J. Cult. Herit.* 22 (2016) 1066–1071, <https://doi.org/10.1016/j.culher.2016.06.006>.
- [13] S.M. Adams, M.L. Levitan, C.J. Friedland, High resolution imagery collection for post-disaster studies utilizing unmanned aircraft systems (UAS), *Photogramm. Eng. Rem. Sens.* 80 (12) (2014) 1161–1168, <https://doi.org/10.14358/pers.80.12.1161>.
- [14] A. Ellenberg, A. Kontos, F. Moon, I. Bartoli, Bridge related damage quantification using unmanned aerial vehicle imagery, *Struct. Control Health Monit.* 23 (9) (2016) 1168–1179, <https://doi.org/10.1002/stc.1831>.
- [15] R. Steffen W. Förstner, On visual real time mapping for unmanned aerial vehicles, in: *21st Congress of the International Society for Photogrammetry and Remote sensing (ISPRS)*, 2008, pp. 57–62.
- [16] S. Lagüela, L. Diaz-Vilarino, D. Roca, J. Armesto, Aerial oblique thermographic imagery for the generation of building 3D models to complement Geographic Information Systems, *Proc. of QIRT 14* (2014).
- [17] I. Lizarazo, V. Angulo, J. Rodríguez, Automatic mapping of land surface elevation changes from UAV-based imagery, *Int. J. Rem. Sens.* 38 (8–10) (2017) 2603–2622, <https://doi.org/10.1080/01431161.2016.1278313>.

- [18] S. Lagüela, L. Díaz, D. Roca, H. Lorenzo, Aerial thermography from low-cost UAV for the generation of thermographic digital terrain models, *Opto-Electron. Rev.* 23 (1) (2015) 78–84.
- [19] C. Eschmann, T. Wundsam, Web-based georeferenced 3D inspection and monitoring of bridges with unmanned aircraft systems, *J. Survey Eng.* 143 (3) (2017) [https://doi.org/10.1061/\(asce\)su.1943-5428.0000221](https://doi.org/10.1061/(asce)su.1943-5428.0000221), 04017003.
- [20] G. Dall’O, L. Sarto, A. Panza, Infrared screening of residential buildings for energy audit purposes: results of a field test, *Energies* 6 (8) (2013) 3859–3878.
- [21] R. Albatici, A.M. Tonelli, M. Chiogna, A comprehensive experimental approach for the validation of quantitative infrared thermography in the evaluation of building thermal transmittance, *Appl. Energy* 141 (2015) 218–228.
- [22] D. Gonzalez-Aguilera, S. Lagüela, P. Rodriguez-Gonzalvez, D. Hernandez-Lopez, Image-based thermographic modeling for assessing energy efficiency of building facades, *Energy Build.* 65 (2013) 29–36.
- [23] M. Mahmoodzadeh, V. Gretka, K. Hay, C. Steele, P. Mukhopadhyaya, Determining overall heat transfer coefficient (U-value) of wood-framed wall assemblies in Canada using external infrared thermography, *Build. Environ.* 199 (2021) 107897, <https://doi.org/10.1016/j.buildenv.2021.107897>.
- [24] M. Mahmoodzadeh, V. Gretka, I. Lee, P. Mukhopadhyaya, Infrared thermography for quantitative thermal performance assessment of wood-framed building envelopes in Canada, *Energy Build.* 258 (2022) 111807, <https://doi.org/10.1016/j.enbuild.2021.111807>.
- [25] J. Ortiz-Sanz, M. Gil-Docampo, M. Arza-García, I. Cañas-Guerrero, IR thermography from UAVs to monitor thermal anomalies in the envelopes of traditional wine cellars: field test, *Rem. Sens.* 11 (12) (2019) 1424, <https://doi.org/10.3390/rs11121424>.
- [26] N. Vorajee, A.K. Mishra, A.K. Mishra, Analyzing capacity of a consumer-grade infrared camera in South Africa for cost-effective aerial inspection of building envelopes, *Front. Architect. Res.* 9 (3) (2020) 697–710, <https://doi.org/10.1016/j.foar.2020.05.004>.
- [27] S. Oh, S. Ham, S. Lee, Drone-assisted image processing scheme using frame-based location identification for crack and energy loss detection in building envelopes, *Energies* 14 (19) (2021) 6359, <https://doi.org/10.3390/en14196359>.
- [28] Ficapal, Mutis, Framework for the detection, diagnosis, and evaluation of thermal bridges using infrared thermography and unmanned aerial vehicles, *Buildings* 9 (8) (2019) 179, <https://doi.org/10.3390/buildings9080179>.
- [29] N. Bayomi, S. Nagpal, T. Rakha, J.E. Fernandez, Building envelope modeling calibration using aerial thermography, *Energy Build.* 233 (2021) 110648, <https://doi.org/10.1016/j.enbuild.2020.110648>.
- [30] J. Kelly, N. Kljun, P.-O. Olsson, L. Mihai, B. Liljeblad, P. Weslien, L. Klemedtsson, L. Eklundh, Challenges and best practices for deriving temperature data from an uncalibrated UAV thermal infrared camera, *Rem. Sens.* 11 (5) (2019) 567, <https://doi.org/10.3390/rs11050567>.
- [31] Ribeiro-Gomes, Krishna David Hernández-López, José F. Ortega, Rocío Ballesteros, Tomás Poblete, Miguel A. Moreno, Uncooled thermal camera calibration and optimization of the photogrammetry process for UAV applications in agriculture, *Sensors* 17 (10) (2017) 2173.
- [32] Smigaj, M.; Gaulton, R.; Barr, S.L.; Suarez, J.C. Investigating the performance of a low-cost thermal imager for forestry applications. In Proceedings of the Image and Signal Processing for Remote Sensing XXII, Edinburgh, UK, 26–28 September 2016.
- [33] H. Zheng, X. Zhong, J. Yan, L. Zhao, X. Wang, A thermal performance detection method for building envelope based on 3D model generated by UAV thermal imagery, *Energies* 13 (24) (2020) 6677, <https://doi.org/10.3390/en13246677>.
- [34] Shweta Dabatwar, Nagesh Kulkarni Nitin, Marco Angelosanti, Christopher Niezrecki, Alessandro Sabato, Sensitivity analysis of unmanned aerial vehicle-borne 3D point cloud reconstruction from infrared images, *J. Build. Eng.* 58 (2022) 105070.
- [35] H. Budzier, G. Gerlach, Calibration of uncooled thermal infrared cameras, *J. Sens. Sensor Syst.* 4 (1) (2015) 187–197, <https://doi.org/10.5194/jsss-4-187-2015>.